Fused silica segments: a possible solution for x-ray telescopes with very high angular resolution like Lynx/XRS

Salmaso, Bianca, Basso, Stefano, Civitani, Marta, Ghigo, Mauro, Hołyszko, Joanna, et al.

Bianca Salmaso, Stefano Basso, Marta Civitani, Mauro Ghigo, Joanna Hołyszko, Daniele Spiga, Gabriele Vecchi, Giovanni Pareschi, "Fused silica segments: a possible solution for x-ray telescopes with very high angular resolution like Lynx/XRS," Proc. SPIE 10399, Optics for EUV, X-Ray, and Gamma-Ray Astronomy VIII, 103990X (8 September 2017); doi: 10.1117/12.2275228

SPIE.

Event: SPIE Optical Engineering + Applications, 2017, San Diego, California, United States

Fused Silica Segments: a possible solution for X-ray telescopes with very high angular resolution like Lynx/XRS

Bianca Salmaso, Stefano Basso, Marta Civitani, Mauro Ghigo, Joanna Hołyszko, Daniele Spiga, Gabriele Vecchi, Giovanni Pareschi

INAF/Brera Astronomical Observatory, Via E. Bianchi 46, 23807 Merate, ITALY

ABSTRACT

In order to look beyond Chandra, the Lynx/XRS mission has been proposed in USA and is currently studied by NASA. The optic will have an effective area of 2.5 m^2 and an angular resolution of 0.5 arcsec HEW at 1 keV. In order to fulfil these requirements different technologies are considered, with the approaches of both full and segmented shells (that, possibly, can be also combined together). Concerning the production of segmented mirrors, a variety of thin substrates (glass, metal, silicon) are envisaged, that can be produced using both direct polishing or replication methods. Innovative post-fabrication correction methods (such as piezoelectric or magneto-restrictive film actuators on the back surface, differential deposition, ion implantation) are being also considered in order to reach the final tolerances. In this paper we are presenting a technology development based on fused silica (SiO_2) segmented substrates, owing the low coefficient of thermal expansion of Fused Silica and its high chemical stability compared to other glasses. Thin SiO_2 segmented substrates (typically 2 mm thick) are figured by direct polishing combined with final profile ion figuring correction, while the roughness reduction is reached with pitch tools. For the profile and roughness correction, the segments are glued to a substrate. In this paper we present the current status of this technology.

Keywords: X-ray telescopes, thin fused silica segments, polishing, super-polishing, ion-beam figuring

1. INTRODUCTION

The future for X-ray telescopes is very challenging: to improve the understanding of the X-ray skies we need optics with very high angular resolution and very large photons collecting area. The superb resolution of Chandra returned images of excellent quality, however, the reduced effective area makes it difficult to operate for spectroscopy of distant sources. The result is that the high-redshift X-ray Universe is still too unresolved to provide us with the understanding of the time evolution of the universe as we see it nowadays. In order to look beyond Chandra, the Lynx mission, previously X-Ray Surveyor (XRS), was presented by NASA,[1] in January 2015, in response to the 2020 Decadal Survey. The goal is to combine comparable (or even better) angular resolution with greatly increased photon throughput. Maintaing sub-arcsec resolution over a large effective area, at an affordable cost, is the challenge.

To reach that, a number of efforts are on going worldwide, approaching the goal both with full shells and with segmented mirrors. Full shells are studied at the Marshall Space Flight Center (MSFC[2]), the Smithsonian Astrophysical Observatory (SAO[3]), the Brera Observatory (OAB[4]); segmented mirrors are developed at the Goddard Space Flight Center (GSFC[5]), the North Western University (NU[6]), the Massachusset Institute of Technology (MIT[7]), the Smithsonian Astrophysical Observatory in collaboration with the Pennsilvania State University (SAO-PSU[8]), the Brera Observatory (OAB, this paper) and the Cosine B.V..[9] Many possible substrates are considered (glass, metal, silicon), and post-fabrication correction methods are envisaged to reach the tight tolerances, such as active correction (SAO/PSU[10]), ion implantation (MIT[11]), differential coating deposition (MSFC/XRO[12]), magneto-restrictive film deposition (NU[6]).

The Brera Observatory is developing both the full[4] and segmented optics (this paper) approach, considering that, for the production of a telescope with 3 m diameter, a combination of both approaches could be required.[13] Considering the heritage of the Chandra optics, the process, both for closed shells and segments, foresees a pre-shaping, polishing, and super polishing activity of glass substrates. Few things are peculiar of our approach:

Further author information: (Send correspondence to B.Salmaso)

B.Salmaso: e-mail: bianca.salmaso@brera.inaf.it, Telephone: +39-02-72320428; www.brera.inaf.it

Optics for EUV, X-Ray, and Gamma-Ray Astronomy VIII, edited by Stephen L. O'Dell, Giovanni Pareschi, Proc. of SPIE Vol. 10399, 103990X · © 2017 SPIE · CCC code: 0277-786X/17/$18 · doi: 10.1117/12.2275228

1. the thickness of the substrate: we reduced the substrate thickness by a factor of 10, considering thickness of 2 mm.
2. the glass material: for cost reason we moved from Zerodur to Fused Silica (SiO_2). Compared to other glasses, Fused Silica has lower coefficient of thermal expansion (CTE = 0.59 $10^{-6}K^{-1}$) and higher chemical stability. Actually, for cost reasons also, we do not use the synthetic Fused Silica, but the electrically fused quartz version. The difference is in the inclusions and bubbles, present in the fused quartz in larger extent with respect to the synthetic version. Anyway, this issue is not relevant in a reflecting optics. In particular, Fused Quartz HSQ300, supplied by Heraeus, was used since many years for our full shell research. In the past, and in this paper too, we used the term Fused Silica for simplicity where actually we should use the more correct Fused Quartz.
3. a final process step: Ion Beam Figuring (IBF) is used at the end of the process to correct the remaining errors (few hundred of nanometers) in the low frequency range.

While the full optics research is on going at OAB since many years, driven by OAB and with the support of LT-Ultra for the grinding and polishing,[14] the segmented optics has been started just last year,[15] with processes fully developed in house. This became possible since OAB has acquired a Zeeko polishing machine (IRP, Intelligent Robotic Polisher, 1200 model) since 2015,[16] within the T-REX (Telescope to Reach the EXtreme) project with the aim to support RD and production programs of the optics for the E-ELT. For what concern the IBF, OAB has built its own equipments and software: a small system was commissioned on 1997, while a second one, commissioned on 2014 for large optics, could produce 4 nm rms on a hexagonal Zerodur mirror, 1 m corner to corner.[17]

During last year, we have been working on Fused Silica segmented optics with the goal to test the full process, from polishing to IBF (not tested yet on closed shells). The idea was to understand, and address, all the possible issues during the different processes, before starting the optimisation work on each of them. Extensive tests on flat Fused Silica samples were performed, and the most relevant issues have been already clarified. Glueing and polishing on Wolter I segment was started. The results are very promising and pave the way for a successful technology development.

Section 2 presents the procurement strategy for the glass segments. Section 3 describes the processes we are using to reach the final tolerances. An analysis of the tolerable errors is presented in Section 4. The works done on flat and Wolter samples are presented in Sections 5 and 6 respectively. Finally our conclusions and outlook are drawn in Section 7.

2. SEGMENTS PROCUREMENT

In this first year of research (phase A), we have been testing the process on segments cut from a closed shell of Fused Quartz (Fig. 1), that accidentally got broken during its processing (shell #7, described in previous paper,[14] with polynomial mirror design, total shell length = 200 mm, diameter at intersection plane (IP) = 487 mm, focal length = 5000 mm). Few segments could be cut with azimuthal span of 100 mm, using the MDI Penett® scribing tool, with wheel in Tungsten Carbide. After the cutting, the segments were found to be deformed from their original shape, with parameters slightly different from the ones previously reported. The Wolter I, that best fit the segment, was used as reference shape for the polishing process.

Actually, the second phase (phase B, adopted when we have demonstrated the capability of the entire process) will have to consider a refined segment procurement, where cost and availability on the market will drive the choice on the following three possibilities:

1. cut the segments from tubes, grind and lap them before starting the polishing process (Fig. 2-top);
2. procure a blank to be ground and lapped (for diameter that cannot be produced in tubes) (Fig. 2-top);
3. pre-slump and if necessary grind and lap the segments (Fig. 2-bottom).

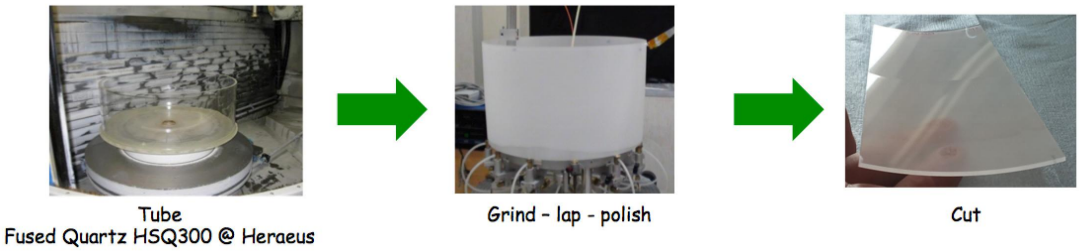

Figure 1. *: Segments procurement in phase A.*

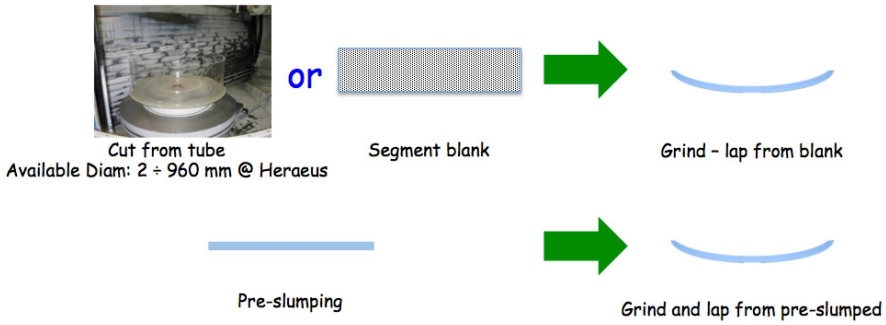

Figure 2. *: Segments procurement in phase B.*

Pre-slumping is at the moment our favourite choice, as it would limit the waste material. OAB has large experience in slumping,[18] but the limit for our furnaces is 950 ℃, while the required temperature to slump the Fused Silica is around 1200 ℃ (see Table 1). Therefore we are exploring the feasibility of pre-slumping the Fused Silica/Quartz, both in terms of requirements and cost, with external partners.

As a last option, we are also considering the possibility to do hot slumping in OAB on borosilicate glass, owing the lower transition temperature (Table 1). Of course the material for the supporting and interfacing structures should match the CTE of the chosen substrate.

Table 1. *Some parameters of different types of glasses (Fused Quartz is the electrically fused version).*

	Fused Silica	**Fused Quartz**	**Borofloat 33**	**D263**	**BK7**
Provider	Heraeus	Heraeus	Schott	Schott	Schott
CTE [10^{-6} K^{-1}]	0.59	0.59	3.25	7.2	7.1
Annealing T [℃]	1100	1220	560	557	557
Density [g/cm^3]	2.2	2.2	2.2	2.51	2.51
Young modulus [GPa]	72.5	72.5	64	72.9	82
Thermal conductivity [W/(mK)]	1.38	1.38	1.2		1.114
Available thk [mm]	0.3-0.5	0.3-0.5	0.70-1.10	0.4-0.7	1-2-3
	1-2...any	1-2...any	1.75-2-2.25...	1.1 (others)	..any

3. THE PROCESS

The figuring equipments are all available in OAB laboratories. The first step is done by bonnet polishing on the 1200 model of the IRP (Intelligent Robotic Polisher) series machine made by Zeeko Ltd. in UK; the spatial frequencies error not correctable by bonnet polishing can be smoothed out in a second step (super-polishing) by equipping the robotic arm with tailored pitch tools or by mounting the pitch tool on a lapping machine also present in OAB laboratories; the third and last step is accomplished by the Ion Beam Figuring (IBF) process, to

remove the remaining few hundred of nanometers in the low frequency range. In this process, it is very important for the IBF to preserve the quality of the surface roughness, already reached with the previous super-polishing step.

The basic idea was already described in a previous paper.[15] The shape of the segment (typically 2 mm thick) is measured in free standing configuration, on a support structure designed to minimise the segment deformation. To figure thin SiO_2 segmented substrates, we have to glue them to a rigid support, both for polishing (with bonnet) and super polishing (with pitch tool). The free standing error map is used as input correction. The segment is then unglued to undergo the last IBF process, present at the end to correct eventual low frequency errors introduced during the previous processes.

We are working at the moment on Wolter I shaped segment. Despite the difficulties in the metrology and the polishing processes of the joined parabola and hyperbola segments, we are working with this configuration for the great simplification in the integration process. Most of the difficulty was found so far in the metrology of the free standing segment, since the repeatability was found not to be satisfactory. Still, we decided to keep working on Wolter I segments, being confident to solve the metrology issue. Therefore, the first polishing test on Wolter I segment, described in Section 6, was performed using the glued error map. We keep on working with the joined configuration on the best effort base.

The different steps of the described process were tested on flat Fused Silica wafers (with thickness of 1 mm, Fig. 3-left, Section 5) and started on Wolter I segments (thickness of 2 mm, Fig. 3-right, Section 6).

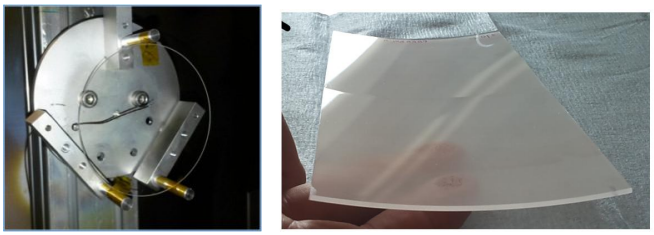

Figure 3. *Left: Flat Fused Silica wafer with thickness of 1 mm and diameter of 100 mm. Right: Wolter I Fused Quartz segment with thickness of 2 mm.*

4. TOLERANCES

A first preliminary work was performed, to understand the allowed tolerances in the segment production, to have a 0.5 arcsec optic. Our reference was the Chandra optics, that was interferometrically measured in the longitudinal direction (the most important in grazing incidence X-ray optics), with rms of the longitudinal profiles being lower than 140 $\AA$, and with tolerable amplitude decreasing with spatial wavelength.[19] The accuracy of the interferometer used for the shape metrology was 220 $\AA$ for the sag over the 840 mm length, and 15 $\AA$ for the remaining figure errors (from 840 to 1 mm).

Our study was devoted to understand which tolerable amplitudes could be accepted in the case of Lynx. To this end, we have computed the expected Half Energy Width (HEW) using the code developed by Raimondi & Spiga,[20] which is implementing physical optics in an idl routine. The HEW was computed in double reflection at 1 keV. Two sets of parameters were used in the calculation (Table 2), describing the segments we are actually working on, and the Lynx case.

Table 2. *Comparison of the optical parameters, used in the HEW computation, for the OAB segments and the Lynx optics.*

	OAB Segments, phaseA	**Lynx**
Diameter at IP [mm]	486	3000
Focal length [mm]	4800	10000
Optical length per side, Par & Hyp [mm]	90	100
Gap per side (non optical region from IP to optical surface) [mm]	5	0

At first, we have considered single harmonics in the Par & Hyp length. Fig. 4-left shows the result for the sag error, that is for an harmonic with spatial wavelength double than the Par & Hyp length. The graph shows that an amplitude of 250 nm would produce 10 arcsec HEW, while 10 nm amplitude would give 0.3 arcsec. Considering harmonics with decreasing SPatial Wavelength (SPW, from 180 mm down to 5 mm) the tolerable amplitude is decreasing accordingly (Fig. 4-right). The non linear behaviour of the curves in this graph is due to the fact that we are considering single harmonics, which do not exists in reality.

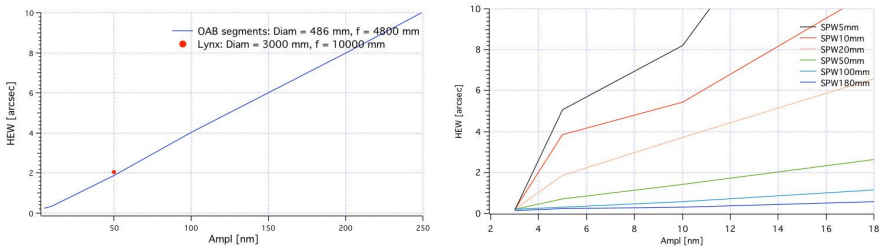

Figure 4. *Single harmonics case. Left: HEW values computed for different amplitudes for an harmonic with spatial wavelength double than the Par & Hyp length. Right: HEW values computed for various spatial wavelengths to show the decreasing tolerable amplitude with decreasing spatial wavelength (OAB segments parameter have been used in this computation).*

A more realistic case can be obtained considering a combination of harmonics: we have obtained a possible profile with a combination of 14 harmonics, from the Par & Hyp length value down to 1 mm. Also different phases were introduced. Two cases were considered, where the harmonics have slope errors of 0.2 and 0.1 μrad. The two Power Spectal Densities (PSDs) are shown in Fig. 5-left, while Fig. 5-right presents a possible profile for the two cases.

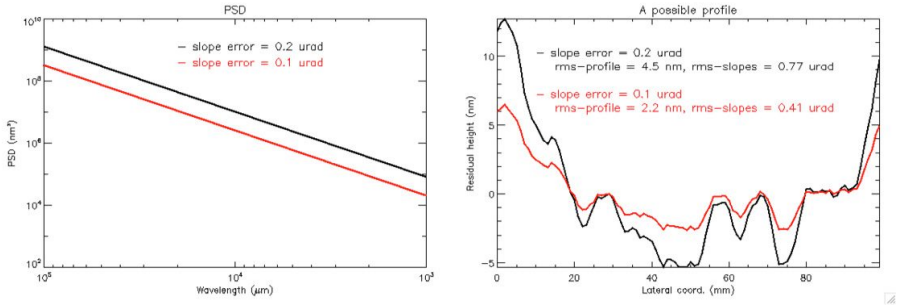

Figure 5. *: Combination of harmonics: a more realistic case. Left: PSD for harmonics with slope errors of 0.2 and 0.1 μrad. Right: Two possible profiles, showing the rms of the profiles and the rms of their slope errors.*

For harmonics with slope errors of 0.2 μrad, we are still above the 0.5 arcsec requirement for the Lynx case (Table 3), while with harmonics of 0.1 μrad slope error we are within tolerances in both cases. A possible profile with slope errors of 0.1 μrad would have rms of 22 $\mathring{A}$, to be compared with the 140 $\mathring{A}$ of Chandra. The lower value is due to the shorter length of the optics (the computation as been checked with the Chandra parameter).

Table 3. *HEW values, computed with physical optics, for a possible longitudinal profile obtained by combining 14 harmonics with slope errors of 0.2 and 0.1 μrad and random phases.*

Slope error	**HEW for OAB Segments, phaseA**	**HEW for Lynx**
0.2 μrad	0.33 arcsec	0.79 arcsec
0.1 μrad	0.17 arcsec	0.27 arcsec

For a clear understanding, we point out that an harmonics with slope error of 0.1 μrad would have amplitude of 5 nm for SPW = 100 mm, and 1 $\mathring{A}$ for SPW = 1 mm, that is extremely challenging.

5. FLAT WAFERS

Flat Fused Silica wafers, with thickness of 1 mm and diameter of 100 mm, were purchased from Edmund Optics. They are provided with clear aperture of 85 % and surface roughness less than 10 $\mathring{A}$. One wafer was used to test the polishing (Section 5.1), super-polishing (Section 5.2) and IBF (Section 5.3). Two other samples were used to solve a roughening issue observed after IBF on Wolter I segments (Section 6)

5.1 Polishing

The wafer was measured with our ZYGO interferometer in a free standing configuration. Our ZYGO GPI-XP, is a Fizeau type interferometer, with He-Ne light source, which provides a flat wavefront with 100 mm diameter. The accuracy of the instrument is $\lambda/100$ (= 6 nm); the rms repeatability is $\lambda/2000$ at 2σ (= 3 Å).

The wafer was then glued on a flat steel support using the Norland Blocking Adhesive NBA107 (Section 6.2).

The Zeeko IRP-1200 polishing equipment, operating in our lab, was used to polish the flat Fused Silica sample. The Zeeko polishing tool is a rubber membrane of spherical shape, named bonnet. The bonnet is inflated by air pressure and covered with polishing pad such as polyurethane foils. Slurry of abrasive particles are projected through a nozzle towards the surface to be polished.

The free standing map was used as input correction. Three runs could reduce the sample Peak to Valley (PV) from 10 to 1 μm (Fig. 6). When unglued, the PV was found to be about 600 nm, lower than the final glued PV, as the input error map was in fact the unglued one.

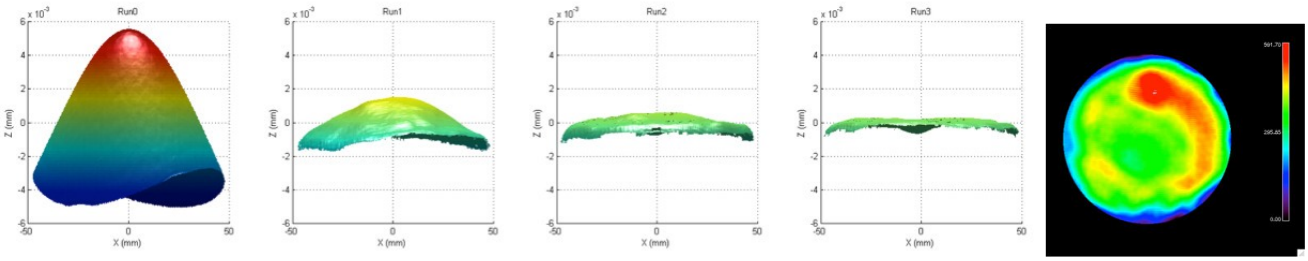

Figure 6. *Interferometric maps of the flat Fused Silica wafers, during polishing with bonnet tool on Zeeko IRP-1200: free standing map used as input correction. Left 4 maps: Glued wafer. PV-start = 10.5 μm, PV-run1 = 3.5 μm, PV-run2 = 1.9 μm, PV-run3 = 1.1 μm. Right: Free standing map after run3. PV = 592 μm, rms = 99 nm.*

A further polishing step was performed to reduce the micro-roughness. We measured the micro-roughness with the Micro Finish Topographer (MFT) installed in our laboratories, a phase shift interferometer equipped with several objectives. The Zeeko pole-down configuration (bonnet tool perpendicular to the surface to be polished) could reduce the roughness from 5-6 nm, after run 3, down to 2.7 nm (Fig. 7).

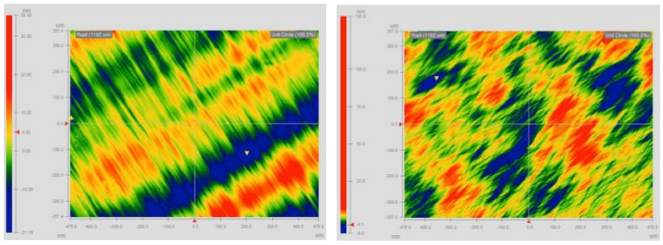

Figure 7. *Polishing with bonnet tool on Zeeko IRP-1200: roughness improvement with pole-down configuration. Roughness is measured with MFT 10×. Left: after run3 rms = 5-6 nm. Right: after run4 (pole down adopted) rms = 2.7 nm.*

5.2 Super-polishing

Super-polishing runs were performed, after the Zeeko runs, to remove some of the errors introduced by the Zeeko itself, in particular the spatial wavelength of 1 mm and the roughness still too high. The super-polishing was

performed on a lapping machine, present in our laboratories, equipped with a pitch tool, using Trizact[21] as abrasive. The process was tested in two areas, one vertical and one horizontal (areas within the green dotted lines in Fig. 8-left). The wavelength of 1 mm (Zeeko fingerprints, visible in the black line of Fig. 8-centre) was clearly removed by Trizact (blue line of Fig. 8-centre). Actually the process was not optimised yet for all mid to high frequencies, therefore some mid frequency errors with larger spatial wavelength were introduced. A very good result, obtained during super-polishing with Trizact, was the improvement of the micro-roughness from 2.7 nm down to 0.6 nm (Fig. 8-right).

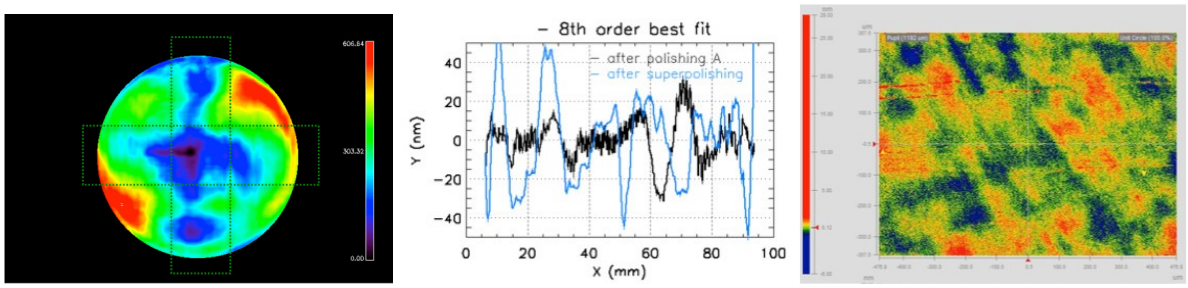

Figure 8. *Superpolishing with pitch tool and Trizact; only the vertical and horizontal portions, inside the green dashed lines, were processed. Left: interferometric image after all runs with Trizact. Center: Comparison of two vertical profiles obtained from the map after Zeeko (Fig. 6-right, black line) and after Trizact (this Figure-left, blue line). Right: roughness after Trizact measured with MFT 10×, rms = 0.6 nm.*

5.3 IBF

The rms of the free standing wafer was 99 nm after Zeeko (Fig. 6-left) and 118 nm after super-polishing (Fig. 8-left), with low and mid frequency errors introduced during the super-polishing itself. While low frequency were expected, mid frequency errors were unwanted and due to a super-polishing process not yet optimised.

We have performed IBF runs to test the process with thin Fused Silica wafers. The sample was positioned at a distance of 60 mm from the IBF source for the following reasons:

1. it was determined to be the focal point of the beam, by images recorded during previous experiments;
2. the distance was also in accordance with tests performed to solve a roughening problem (Section 6.1) observed on Fused Silica samples positioned at the 36 mm distance, typically used in our laboratories until now (and causing no problems on samples other than Fused Silica).

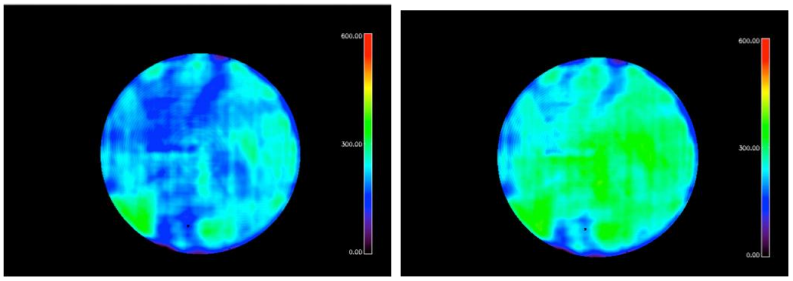

Figure 9. *IBF: interferometric images after 3 runs. Left: piston, tilt and power removed, rms = 39 nm. Right: piston, tilt removed, rms = 46 nm.*

The overall shape was improved to about 40 nm rms (Fig. 9) after 3 IBF runs. A curvature error (convex) was actually found to be introduced by the IBF: in fact, the raw map after IBF (Fig. 9-right) have rms of 46 nm with a convex deformation of the glass, confirmed by measurements on the back side. The mathematical subtraction of a power error did reduce the rms to 39 nm (Fig. 9-left).

This glass deformation was unexpected, as the maximum temperature reached during the IBF, measured by a thermocouple touching the back surface, was about 100 ℃, far below the fused silica transformation temperature (Table 1). To address this problem, we plan to simulate the stress deformation induced by IBF via FEM and possibly introduce it in the IBF correction. Also the effect on 2 mm thick samples have to be checked.

6. WOLTER I SEGMENTS

A preliminary result on Wolter I Fused Silica segment was presented last year.[15] The segment (named segment A, from here on) had a quite large PV error, but relatively small mid frequency, as it was already partially polished within the closed shell program.[14] It was processed with the IBF facility, in order to impart the correct Wolter I shape, reducing the expected HEW of the longitudinal profiles from 46 to about 1 arcsec.[15]

To continue the work on Wolter I segments, we have performed two sets of works:

1. segment A was found, after IBF, covered by peaks degrading the roughness: IBF tests, again on flat wafers, were performed to solve the problem (Section 6.1);
2. a new segment (named segment B, from here on) was glued to a solid support (Section 6.2) and polished with the Zeeko equipment (Section 6.3) to test the processes.

6.1 Solving the roughness issue after IBF

The optical surface of the Fused Silica segment A, was found, after the IBF process, covered by peaks (Fig. 10-left) of material that was determined to be Fused Silica by SEM micro-analysis. The roughness of this sample, measured with MFT 10×, increased from 1 nm before IBF to 2.2 nm after IBF (black line in Fig. 10-right). The IBF was performed holding the sample at a distance of 36 mm from the ion source. To mitigate the problem, two additional Fused Silica flat samples were processed with IBF at 36 and 70 mm distance. The sample 1, processed at the closest distance (36 mm from the IBF source, red line in Fig. 10-right), was processed with the same parameter of the Wolter I segment A. The PSDs of these two samples (Samples 1 and 3) were compared with the PSD obtained from a brand new Fused Silica sample (Sample 2, green line in Fig. 10-right), proving a 70 mm distance (Sample 3, orange line in Fig. 10-right) as appropriate to minimize the problem.

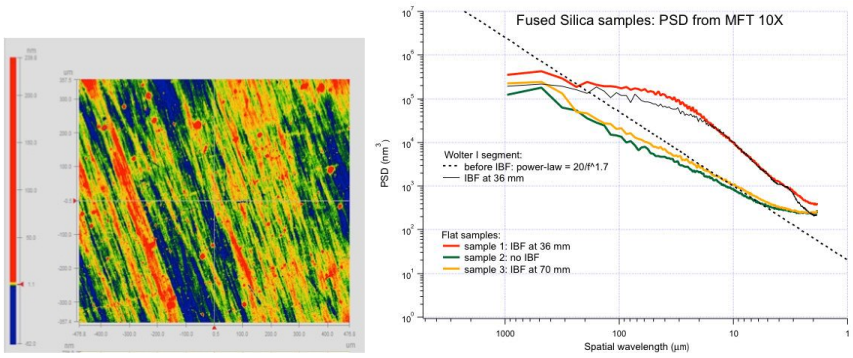

Figure 10. *Roughness mitigation after IBF. Left: MFT 10× image taken on segment A after IBF performed at 36 mm distance from the source (rms = 2.2 nm). The roughness of this sample, before IBF, was 1 nm rms on the same spatial wavelength range. Right: the PSD from roughness measurements taken with the MFT 10×. The PSD of segment A, processed with IBF at 36 mm distance from the source, (black line) matches the PSD of the flat sample #1, also processed at 36 mm distance (red line). The PSD of the sample #3, processed at 70 mm distance, almost matches the PSD of the brand-new sample #2. The dotted black line corresponds to the power law that best fits the roughness of the segments before the IBF process.*

X-Ray scattering measurements were also performed with the BEDE-D1 equipment, present in OAB laboratories, on the Fused Silica flat samples previously processed with the IBF at different distances from the source,

and the sample kept unprocessed as reference. The goal was to confirm that the peaks, observed on the sample processed at 36 mm distance, would produce X-ray scattering.

The BEDE-D1 diffractometer was used in the monochromatic mode of 8.045 keV (Cu-Kα line). We were really interested in the assessment of scattering at 1 keV, so at 8.045 keV we had to use an incidence angle smaller than the nominal one (315 arcsec versus a nominal of 0.71 deg) in order to keep the ratio $\lambda/\sin\theta_{inc}$ (hence the scattering) at the same value .

The samples were found to produce scattering to an extent dependent on their roughness (Fig. 11-left), and the XRS level turned out to be in agreement with the PSD computed from the MFT maps (Fig. 11-right). In particular, Sample 1, the one with the highest roughness and with the highest density of peak defects in the topographic maps, returned the highest scattering level and the PSD computed from the XRS diagrams was in agreement with MFT measurements. Since the peaks represent the dominant term of the PSD degradation, we conclude that the peaks present on the surfaces do contribute to the X-ray scattering, as per the 1st order scattering theory. Moving the sample from 36 to a 70 mm distance does reduce the roughness and therefore the scattering.

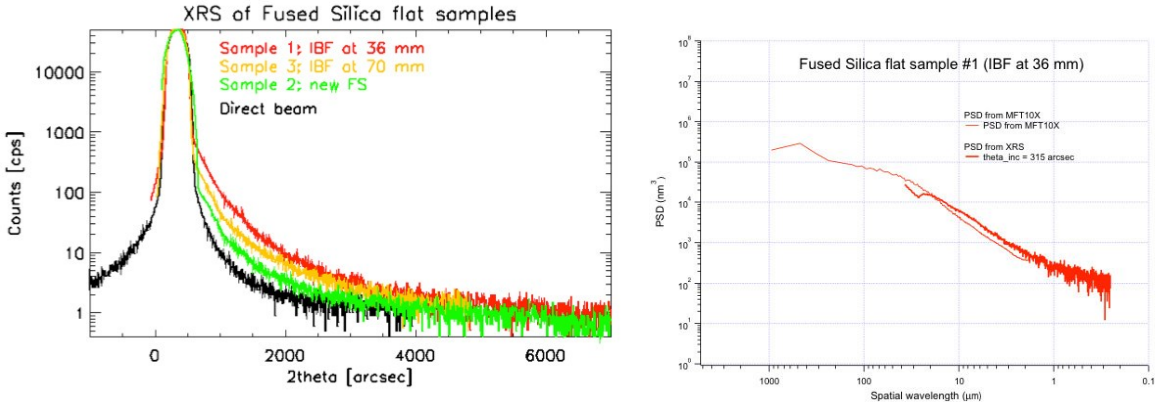

Figure 11. *Left: XRS scans at 8.045 keV and 315 arcsec incidence angle of the flat Fused Silica samples, compared with the direct beam (black line). The red line is sample #1, processed with the IBF source at 36 mm distance. The orange line was obtained from sample #3, processed with the IBF source at 70 mm distance. Green line represents the sample #2, the only unprocessed sample. Right: matching of the PSD computed from an XRS measurement at 315 arcsec incidence angle and the PSD computed from the roughness data obtained with the MFT 10×, for the Sample #1.*

6.2 Glueing

For the polishing and super-polishing processes, we glue the samples (both flat and Wolter I) to a rigid support. For the Wolter I sample, we have first realised an aluminium support with double cone profile and thickness of 10 mm. We then moved to a thicker support (40 mm) to minimise thermal effects during the glueing.

Two glueing solutions were studied:

1. Norland Blocking Adhesive NBA107. This is a UV curing adhesive specifically formulated to provide low shrinkage (1.5%) and low strain (tensile strength = 76 psi). The adhesive cures by exposure to UV light in the range of 350 to 380 nanometers. The adhesive needs 5 joules per centimeter squared of long wave UV energy to fully cure. Debonding is accomplished by soaking parts in a soapy warm (80 ℃) water solution (or acetone).
2. a blocking wax with melting point between 36 and 42 ℃.

Segment A was measured, before and after glueing with both solutions, on our Long Trace Profilometer (LTP) to precisely assess the mid frequency errors on the central scan: a best fit 8th order polynomial was subtracted from the raw profiles the make the mid frequencies visible. Fig. 12 shows that the UV glue (red curve) introduces mid frequencies with higher amplitude with respect to the blue wax (blue curve), while the errors intrinsic in

the sample (black line) elastically recover their amplitude after debonding (green line). Despite we are not sure if these mid frequency would be a problem or not (as we intend to work on the free standing error map), we have chosen to do the first test on Zeeko with the blue blocking wax. The main reason was to be conservative in our approach; another reason was that the first polishing with Zeeko was actually done on the glued error map (Section 6.3) because of repeatability problems with the free standing metrology still to be solved.

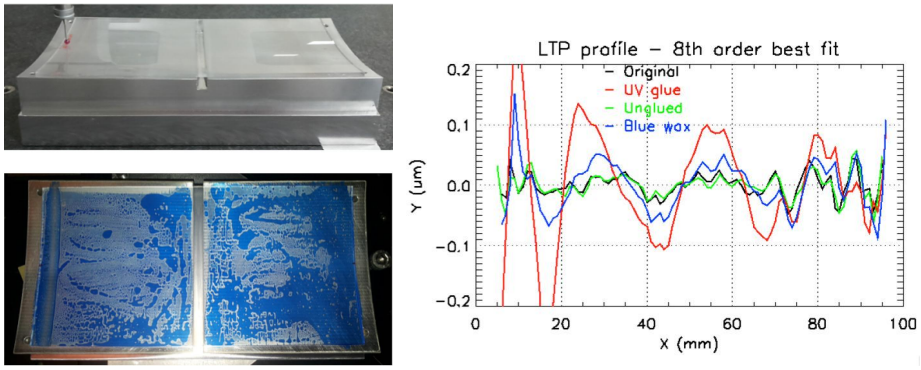

Figure 12. *Glue comparison. Left: at the top, the segment glued on the thick aluminium support with the UV glue; at the bottom, the blue blocking was used. Right: LTP central profiles of the parabola (left side in the photos) after the subtraction of the best fit height order polynomial. Black and green lines are before glueing and after unglueing. Red line is after glueing with UV glue. Blue line is after glueing with the blue blocking wax.*

6.3 Polishing

Segment-B was first measured on our Characterization Universal Profilometer (CUP), glued on a thick aluminium support, in vertical configuration (Fig. 13-left). The blue blocking wax was selected for this step. The segment was cut from the same closed shell of segment A, with polynomial profiles, Diameter at IP = 487 mm and focal distance = 5000 mm. We already noticed with segment A, that the cut deforms the segments: the best free standing measurement of segment A returned diameter = 486 mm and focal = 4920 for the best fitting Wolter. We have therefore designed and realised a support with double cone shape, Diameter at IP = 489 mm (to account for the 2 mm thin segment) and focal = 4900 mm. We are aware that the glueing to this support would also deform, to a smaller extent, the segment; but the basic idea of working on the free standing error map would turn this not to be a problem. The best fitting Wolter for the glued segment B had Diameter at IP = 485.6 mm and focal = 4768 mm.

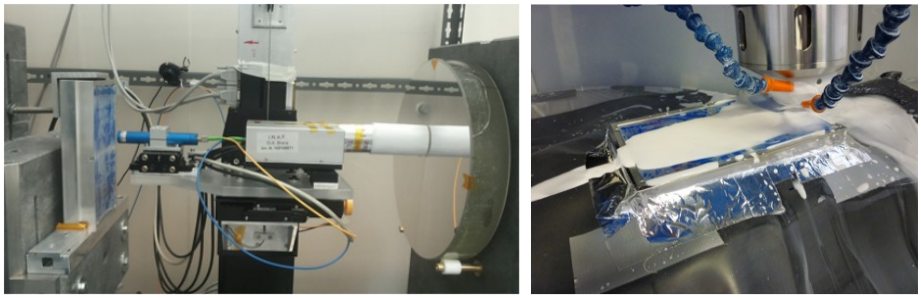

Figure 13. *Left: The Wolter I segment (glued on its aluminium support) during the metrology with CUP. Right: The segment during the polishing with Zeeko.*

The glued error map was used as input error to our Zeeko equipment, and only half of the error was introduced as first trial. The deviation of the segment from nominal was quite large, with PV = 22.7 μm (Fig. 14-left) in the central region with azimuthal span of 70 mm (and also not considering the IP region on a length ± 5 mm. The result is quite positive, with a reduction of the PV down to 12.2 μm (Fig. 14-right) and with an error in the removal input of rms = 658 nm. We expect a reduction to 50 nm rms after 4 runs.

In order to reduce the polishing errors and the Zeeko processing time, for the segment procurement of phase B we plan to adopt a maximum deviation from nominal of 10 μm PV.

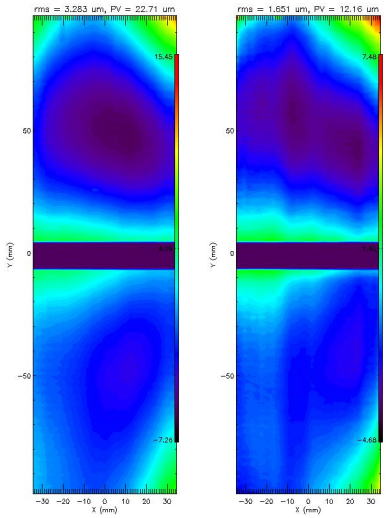

Figure 14. *Error maps of segment B, as measured with our CUP. The azimuthal central area of 70 mm was polished and shown. Left: before Zeeko. Right: after Zeeko.*

7. CONCLUSIONS AND OUTLOOK

In this paper we have presented a new process based on direct polishing and ion figuring correction of thin Fused Silica segments, for the realisation of an X-ray telescope like the one foreseen for the Lynx mission, with an angular resolution similar to Chandra but with much larger effective area.

An analysis of the tolerable errors was performed using physical optics. In order to have HEW lower than 0.5 arcsec, the longitudinal profiles should include harmonics with slope errors of 0.1 μrad, which means amplitude of 5 nm for spatial wavelength of 100 mm and 1 $\AA$ for spatial wavelength of 1 mm: very challenging both for the production process and the metrology.

The entire procedure (glueing, polishing, super polishing and ion figuring) has been tested on flat Fused Silica wafers 1 mm thin:

1. the polishing with our Zeeko IRP1200 improved the figure from 10 μm to about 600 nm PV; the pole-down configuration decreased the roughness from 5-6 to 2.7 nm rms;
2. the super polishing with pitch tool and Trizact as abrasive, performed on our lapping machine, removed the 1 mm spatial wavelength errors introduced during the polishing step. The roughness was improved from 2.7 to 0.6 nm rms. Being the process not fully optimised, unwanted mid frequency errors were introduced that were partially corrected by the following step;
3. the final Ion Figuring could reduce the shape rms from 118 to about 40 nm. A small convex deformation was observed after IBF correction, and this deformation was confirmed by measurements on the back side of the wafer, performed before and after IBF.

Preliminary results obtained on Wolter I segments are very encouraging:

1. the roughening observed after IBF on a previous segment, processed with a distance of 36 mm from the ion source, was solved by placing the sample at a larger distance from the source;
2. two different glueing solutions were studied (UV glue and blocking wax) and, at the moment, the wax was selected to minimise mid frequency deformations introduced by the glueing process;

3. a first polishing with our Zeeko IRP1200, using the glued error map as input, in the measure of half of the total error, could reduce the PV from 22.7 down to 12.2 μm.

After this overall look into the entire process, we plan to: optimise the super-polishing process; understand and correct the convex deformation introduce on 1 mm thin wafers, possibly introducing in the IBF correction the deformation computed with FEM; continue the polishing with Zeeko on the glued segment. The key point still to be optimised is the measurement of the segment in free standing configuration. For the moment, we keep working with the Wolter I configuration on a best effort base.

ACKNOWLEDGMENTS

We kindly thank ICMATE-CNR-Lecco for the SEM microanalysis of the Fused Silica segments after IBF, and Zeeko Ltd for the support on the polishing of Wolter I segments.

REFERENCES

[1] Gaskin, J.A., et al., "The X-ray Surveyor mission: a concept study," Proc. SPIE 9601, 96010J (2015)
[2] Gubarev, M.V., et al., "Development of the a direct fabrication technique for full-shell x-ray optics," Proc. SPIE 9905, 99051V (2016).
[3] Romaine, S., et al., "Miniature Lightweight X-ray Optics (MiXO) and CubeSat X-ray Telescope (CubeX) for solar system exploration," Proc. SPIE 10399, this conference (2017)
[4] Civitani, M.M., et al., "Thin fused silica shells for high-resolution and large collecting area x-ray telescopes (like Lynx/XRS)," Proc. SPIE 10399, this conference (2017)
[5] Riveros, R.E., et al., "Progress on the fabrication of lightweight single-crystal silicon x-ray mirrors," Proc. SPIE 10399, this conference (2017)
[6] Ulmer, M.P. et al., "Controlling the shaping of Si and glass substrates via stresses in the coatings: via bias stress control and magnet fields," Proc. SPIE 10399, this conference (2017)
[7] Zuo, H., et al. "Recent progress on experiments and numerical analysis of air bearing slumping for x-ray telescope mirror substrates," Proc. SPIE 10399, this conference (2017)
[8] Cotroneo, V., et al., "Thermal forming of glass substrates for adjustable optics," Proc. SPIE 10399, this conference (2017)
[9] Collon, M.J., et al., "Development of the Athena mirror modules," Proc. SPIE 10399, this conference (2017)
[10] Allured, R., et al., "Deterministic figure correction of piezoelectrically adjustable slumped glass optics," Proc. SPIE 10399, this conference (2017)
[11] Chalifoux, B.D., et al. "Effects of ion implantation in different substrate materials: stress, relaxation, and strength," Proc. SPIE 10399, this conference (2017)
[12] Kilaru, K., et al., "Improving x-ray optics via differential deposition," Proc. SPIE 10399, this conference (2017)
[13] Basso, S., et al., "A hybrid concept (segmented plus monolithic fused silica shells) for a high-throughput and high-angular resolution x-ray mission (Lynx/XRay Surveyor like)," Proc. SPIE 10399, this conference (2017)
[14] Civitani, M.M., et al., "Thin monolithic glass shells for future high angular resolution and large collecting area x-ray telescope," Proc. SPIE 8884, 88841R (2013)
[15] Pareschi, G., Basso, S., Civitani, M., Ghigo, M., Parodi, G., Pelliciari, C., Salmaso, B., Spiga, D., Vecchi, G., "Beyond Chandra (towards the X-ray Surveyor mission): possible solutions for the implementation of very high angular resolution X-ray telescopes in the new millennium based on fused silica segments," Proc. SPIE 9905, 99051T (2016)
[16] Vecchi, G., et al., "A bonnet and fuid jet polishing facility for optics fabrication related to the E-ELT," Mem. S.A.It. 86, 408 (2015)
[17] Ghigo, M. , Vecchi, G. , Basso, S. , Citterio, O. , Civitani, M. , Mattaini, E., Pareschi, G. , Sironi, G., "Ion figuring of large prototype mirror segments for the E-ELT," Proc. SPIE 9151, 91510Q (2014)

[18] Salmaso, B., Basso, S. Civitani, M.M., Ghigo, M., Holyszko, J., Spiga, D., Vecchi, G., Pareschi, G., "Slumped Glass Optics development with pressure assistance," Proc. SPIE 9905, 990523 (2016)

[19] Gordon, T.E., Catching, B.F., "Status of the Advanced X-ray Astrophysics Facility (AXAF) Optics Production Program," Proc. SPIE 2263, 233-242, (1994)

[20] Raimondi, L., Spiga, D., "Mirror for X-ray telescopes: Fresnel diffraction-based computation of point spread functions from metrology," AA 573, A22 (2015)

[21] http://multimedia.3m.com/mws/media/352831O/ab0205-gamma-trizact.pdf